JACC: CARDIOVASCULAR IMAGING VOL. 4, NO. 7, 2011

ISSN 1936-878X/$36.00
PUBLISHED BY ELSEVIER INC. DOI:10.1016/j.jcmg.2011.03.018

Feasibility and Acute Efficacy of Radiofrequency Ablation of Cavotricuspid Isthmus–Dependent Atrial Flutter Guided by Real-Time 3D TEE

François Regoli, MD, PhD,* Francesco F. Faletra, MD,* Gaetano Nucifora, MD,* Elena Pasotti, MD,* Tiziano Moccetti, MD,* Catherine Klersy, MD,† Angelo Auricchio, MD, PhD*
Lugano, Switzerland; and Pavia, Italy

OBJECTIVES The aim of this study was to evaluate the feasibility and acute efficacy of real-time 3-dimensional transesophageal echocardiography (RT3DTEE)–guided ablation of the cavotricuspid isthmus (CVTI).

BACKGROUND The use of RT3DTEE to guide a transcatheter radiofrequency ablation procedure has never been systematically investigated.

METHODS Seventy consecutive patients with CVTI-dependent atrial flutter underwent CVTI ablation. Procedural monitoring using RT3DTEE was assigned to patients who requested general anesthesia for the procedure (n = 21 [30%]). In the other 49 patients (the control group), the procedures were monitored using the standard fluoroscopic approach. Procedural time was considered as skin-to-skin electrophysiological procedure duration, not including anesthesia preparation; adequate radiofrequency ablation applications (with fixed temperature and power settings) were considered as lesions lasting ≥ 60 s.

RESULTS RT3DTEE allowed visualization of the CVTI and identified related structures in most patients (20 of 21); anatomic features such as long CVTI (n = 11), prominent Eustachian ridge (n = 9), prominent Eustachian valve (n = 6), septal recess (n = 8), and pectinate muscles (n = 10) were frequent. Also, RT3DTEE allowed continuous visualization of ablation catheter movement and contact. Compared with the control group, RT3DTEE was equally effective in achieving CVTI bidirectional block (100% in both groups), and no complications occurred. RT3DTEE shortened procedural time (median 73.0 min, interquartile range [IQR] 60.0 to 90.0 min, vs. median 115.0 min, IQR 85.0 to 133.0 min, $p < 0.001$), reduced radiation exposure (median fluoroscopy time 4.2 min, IQR 3.1 to 8.4 min, vs. median 19.3 min, IQR 12.9 to 36.4 min, $p < 0.001$; median fluoroscopy dose 575.4 cGy · cm^2, IQR 428.5 to 1,299.4 cGy · cm^2, vs. median 3,520.7 cGy · cm^2, IQR 1,700.0 to 6,709.0 cGy · cm^2, $p < 0.001$), and reduced the number of radiofrequency applications to achieve bidirectional block (median 7, IQR 6 to 10, vs. median 12, IQR 10 to 22, $p = 0.007$). A strong learning curve was detected by comparing procedural data between the first and last patients treated using RT3DTEE.

CONCLUSIONS RT3DTEE-guided ablation of CVTI was feasible, allowing real-time detailed morphological CVTI characterization as well as continuous visualization of the ablation catheter during radiofrequency ablation. This approach entailed marked reductions in procedural time, radiation exposure, and the number of radiofrequency applications. (J Am Coll Cardiol Img 2011;4:716–26) © 2011 by the American College of Cardiology Foundation

From the *Division of Cardiology, Fondazione Cardiocentro Ticino, Lugano, Switzerland; and the †Service of Biometry and Clinical Epidemiology, Fondazione IRCCS Policlinico San Matteo, Pavia, Italy. Dr. Faletra has received speaking fees from Philips Medical Systems. Dr. Auricchio is a consultant for Sorin Group, Medtronic, Biotronik, EBR System, Merck,

Radiofrequency ablation (RFA) of the cavotricuspid valve isthmus (CVTI) is a widely applied, highly successful nonpharmacological therapy for atrial flutter (1,2). It is well recognized, however, that varying anatomical and morphological aspects of the CVTI may at times render conduction block across the CVTI through catheter ablation difficult, thus resulting in prolonged ablation and fluoroscopy times or even procedural failure. Continued efforts have therefore been oriented toward developing further innovative ablative (3,4) and mapping (5,6) strategies as well as imaging modalities (7) to ensure incremental procedural success while reducing procedural duration

See page 727

and risk; also, procedure-related biological risk by prolonged exposure to ionization radiation represents a growing concern (8).

Real-time 3-dimensional transesophageal echocardiography (RT3DTEE) is a recently developed technique that provides 3-dimensional images of unprecedented quality. Because the right atrium is close to the transducer, this allows visualization of morphology and anatomy with great detail, as outlined in a recent contribution (9). In the specific context of CVTI ablation, RT3DTEE may help accurately characterize anatomical barriers limiting efficacious RFA delivery. Although RT3DTEE monitoring of pulmonary vein isolation procedure has been reported anecdotally (10), whether RT3DTEE may precisely delineate the CVTI and be suitable for guiding ablation in this region has not been demonstrated so far.

Therefore, the objectives of the present study were 3-fold: 1) to assess the feasibility of RT3DTEE to image the CVTI and evaluate the ability to navigate with the mapping catheter within the CVTI region; 2) to verify the acute efficacy of RT3DTEE-guided CVTI ablation by comparison with the conventional fluoroscopy-guided approach; and 3) to evaluate potential reductions of radiation exposure using RT3DTEE.

METHODS

Patient population. This was a single-center, prospective, observational study including consecutive patients presenting electrocardiographically documented typical atrial flutter who underwent RFA of the CVTI at Cardiocentro Ticino (Lugano, Switzerland). After obtaining patients' written and oral consent to the procedure, and at patients' request, RFA was carried out either with or without deep sedation. When under general anesthesia, patients were monitored using RT3DTEE. Patients in whom CVTI RFA had previously failed or who presented associated atrial tachyarrhythmias with common atrial flutter (atrial fibrillation, atrial arrhythmias, re-entry tachycardia, and so on), were excluded from the study. Between January 2009 and November 2010, 70 consecutive patients underwent isolated, first-time CVTI-dependent atrial flutter ablation. Twenty-one patients (30%) requested general anesthesia (the RT3DTEE group). Patients in whom CVTI ablation was carried out according to the fluoroscopy-based approach represented the control group.

CVTI ablation procedure. In all patients, antiarrhythmic drugs as well as oral anticoagulation therapy were discontinued before the ablation procedure. The ablation procedure was conducted by positioning 2 standard decapolar deflectable catheters via the femoral vein along the right atrial free wall and another in the coronary sinus. A conventional 8-mm mapping ablation catheter was then used. Intracavitary digitalized electrograms and 12-lead surface electrocardiograms were recorded and displayed on a multichannel recorder and stored on magneto-optical discs (Prucka CardioLab; GE Marquette Medical Systems, Milwaukee, Wisconsin). RFA was performed with either EPT-1000 XP (EP Technologies, Mountain View, California) or Cordis-Stockert (Cordis-Webster, Miami Lakes, Florida) radiofrequency (RF) generators, allowing the delivery of continuous, unmodulated current, with power output set at 80 W and a pre-set temperature of 65°C. The end point of the ablation procedure was the achievement of complete bidirectional CVTI block (11,12), persisting for a waiting period of 30 min.

The following procedural data were collected: total procedural time, total RF application time and number of RF applications (applications ≥ 60 s in

ABBREVIATIONS AND ACRONYMS

CVTI = cavotricuspid isthmus
IQR = interquartile range
RF = radiofrequency
RFA = radiofrequency ablation
RT3DTEE = real-time 3-dimensional transesophageal echocardiography

Biosense Webster, BDS Cordis, Philips, Impulse Dynamics, and has received speaker fees from Sorin Group, Medtronic, Biotronik, St. Jude Medical, and Abbott. All other authors have reported that they have no relationships to disclose.

Manuscript received October 10, 2010; revised manuscript received March 7, 2011, accepted March 17, 2011.

JACC: CARDIOVASCULAR IMAGING, VOL. 4, NO. 7, 2011
JULY 2011:716–26

duration [5]), fluoroscopy time, and cumulative exposure dose. Procedural time in the RT3DTEE group did not include anesthesia preparation time but was limited to the duration of the electrophysiological procedure.

Real-time 3-dimensional transesophageal echocardiographic acquisition and analysis. RT3DTEE was performed using a commercially available fully sampled matrix-array transesophageal echocardiographic transducer and ultrasound system (X7-2t Live 3D transducer, iE33; Philips Medical Systems, Andover, Massachusetts). First, a real-time 3-dimensional image from the 2-dimensional 4-chamber plane was obtained, using a pyramidal dataset large enough to include the entire right atrium. Subsequently, by using the auto-crop function, the anterior half of the atrium was removed, and an arbitrary crop was applied to remove remaining nonrelevant anatomic structures. The image was then rotated to provide a perspective similar to the fluoroscopic left anterior oblique view (Fig. 1). From this position, a slight clockwise rotation and a deeper cut of the frontal plane were applied to provide a perspective similar to the fluoroscopic right anterior oblique view. Both views allowed evaluation of the length of the CVTI and the details of its anatomical features (Figs. 2 and 3). Real-time images were viewed by both the echocardiographer and the electrophysiologist during the RFA procedure.

Quantitative analysis of CVTI length was performed offline using dedicated software (QLAB Cardiac 3DQ; Philips Medical Systems). The multiplanar reconstruction mode of the software was used to identify the exact extensions of the right atrial myocardium for accurate CVTI length determination; the length of CVTI was then measured at end-systole as the linear distance between the tricuspid annulus and the end of the right atrial myocardial sleeve.

All remaining qualitative analyses were performed online during the acquisition of real-time 3-dimensional images. In particular, the Eustachian ridge was evaluated as either prominent or normal, while the Eustachian valve was judged as prominent, moderate, or unremarkable. The presence of a septal recess was recorded, and it was assessed as large (when the recess extended to reach the mid-CVTI), regular, or absent. Finally, encroachment of pectinate muscles into the CVTI was determined and reported as abundant, of moderate extent, or absent (Figs. 2 and 3).

Reproducibility of echocardiographic analysis. The datasets of 10 patients were randomly selected and analyzed again 3 months later by the original observer and by a second observer who was blinded to the results of the previous analysis. Intraobserver and interobserver agreement was assessed for the quantitative measurements of CVTI length and for

Figure 1. RT3DTEE and Fluoroscopic Views of the CVTI

Real-time 3-dimensional transesophageal echocardiography (RT3DTEE) allows visualization of anatomical details of the cavotricuspid isthmus (CVTI). AO = aorta; CS = coronary sinus; CVTI = cavotricuspid isthmus; EV = Eustachian valve; LAO = left anterior oblique; RA = right atrium; RAO = right anterior oblique; SVC = superior vena cava; TV = tricuspid valve.

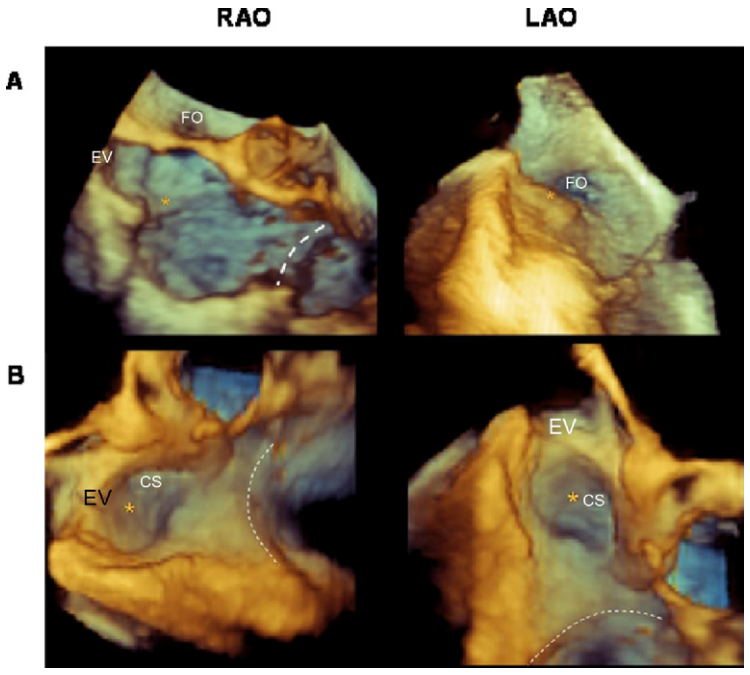

Figure 2. Prominent Anatomical Features of the CVTI

Prominent features include pectinate muscles encroaching from the crista terminalis **(yellow asterisks in A)**, prominent Eustachian valve, and septal recess **(yellow asterisks in B)**. FO = foramen ovale; other abbreviations as in Figure 1.

the qualitative evaluations of the Eustachian ridge, Eustachian valve, septal recess or pouch, and pectinate muscles.

Statistics. Continuous variables are expressed as mean ± SD or as median (interquartile range [IQR]) if appropriate. Normally distributed data were compared using independent Student *t* tests. Otherwise, comparisons between groups were performed using Mann-Whitney *U* tests. Categorical values are stated as absolute and relative frequencies and were compared using Fisher exact tests. All tests were 2 tailed.

Intraobserver and interobserver agreement in the measurements of CVTI length was assessed using Bland-Altman analysis and expressed as the mean difference between the 2 measurements ± 2 SDs. For qualitative evaluation of anatomical features such as the Eustachian valve, kappa statistics were used, and the level of agreement was interpreted as follows: 0 to 0.2 = poor to slight, 0.21 to 0.4 = fair, 0.41 to 0.6 = moderate, 0.61 to 0.8 = substantial, and 0.81 to 1.0 = nearly perfect. A linear regression model for either fluoroscopy time or dose was fitted, including ablation time (log-transformed), group, and their interaction. Stata version 11 (StataCorp LP, College Station, Texas) was used for computation. A p value <0.05 was considered statistically significant.

RESULTS

Comparison of the baseline characteristics between the 2 groups is presented in Table 1. Patients in the control group were significantly older than those in the RT3DTEE group and presented a trend toward slightly lower left ventricular ejection fractions. The prevalence of atrial fibrillation, however, was higher in the RT3DTEE group.

Reproducibility of echocardiographic analysis. Intraobserver and interobserver agreement for the measurement of CVTI length was good; according to Bland-Altman analysis, the mean differences ± 2 SDs for CVTI length were 1.6 ± 4.0 mm and 1.8 ± 7.0 mm, respectively.

Intraobserver and interobserver agreement for the qualitative evaluation of the Eustachian ridge (kappa = 1.0 for both), Eustachian valve (kappa = 1.0 for both), septal recess or pouch (kappa = 0.80 for both), and pectinate muscles (kappa = 1.0 and 0.80, respectively) was nearly perfect.

Feasibility of RT3DTEE to visualize the CVTI. In all but 1 patient (5%), intraprocedural visualization of the CVTI was possible. The reason for failure was a

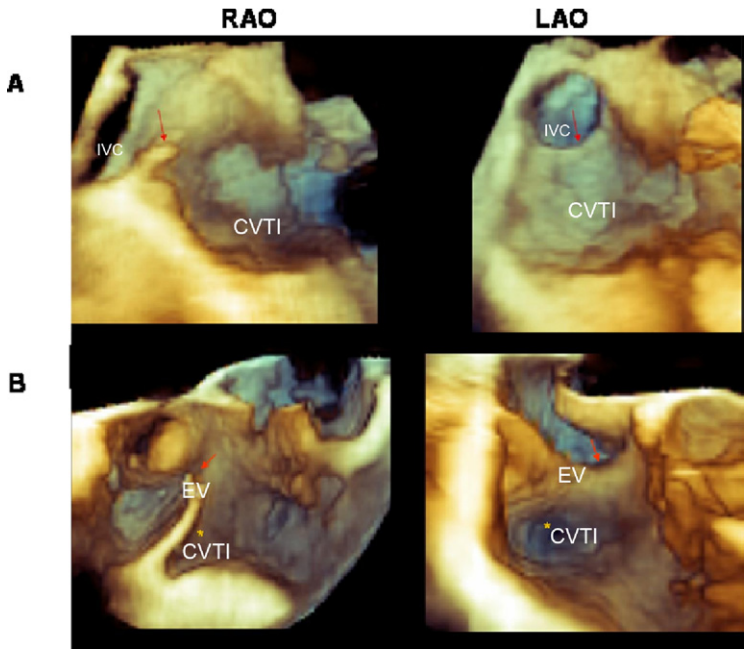

Figure 3. Features of the Septal Portion of the CVTI

A frequently encountered anatomical feature of the cavotricuspid isthmus (CVTI) is a prominent Eustachian valve **(red arrows in A and B)**. Anterior insertion of the valve in the septum may produce a deep septal recess **(yellow asterisks in B)**.

prominent aortic bulb with a marked protrusion into a small-sized right atrium. In the remaining 20 patients, CVTI imaging was always possible, and visualization was considered of good quality in most cases (75%). The median length of the CVTI was 40 mm; in 11 patients (55%), CVTI length was higher than the median value, and it was therefore labeled "long CVTI." With the exception of 2 patients (10%) in whom the CVTIs were found to be morphologically normal, the other 18 patients (90%) presented at least 1 prominent anatomical feature (Table 2).

Feasibility of RT3DTEE to visualize the ablation catheter. RT3DTEE allowed visualization of the mapping catheter when moved from the septal to the lateral position and vice versa (Fig. 4A). Typical drag movement (anterior to posterior movement along the CVTI) could be equally appreciated; however, limited visibility of the catheter tip was encountered when the tip reached the proximal portion of the CVTI, before entering the inferior vena cava. Visualization of catheter tip contact was possible with RT3DTEE in many patients (50%) but was limited by 2 key factors, namely, different acoustic resonance yielded by different catheter manufacturers (Fig. 4A) and acoustic shadowing of the catheter due to the artifact beam (Fig. 4B). These difficulties could be corrected by gentle rotation of the ultrasound probe and adjustment of acoustic gain and cropping or by selecting 1 particular catheter manufacturer (Online Video 1).

Efficacy and safety of the RT3DTEE-guided approach for ablation. Achievement of bidirectional CVTI block was possible in all patients regardless of the monitoring approach (fluoroscopy or RT3DTEE). Patients monitored by RT3DTEE had significantly shorter procedural times and were exposed to significantly less radiation. Also, a smaller median number of RF applications was needed to achieve bidirectional block compared to the control group (Table 3). The association between radiation exposure and ablation time (Fig. 5) was not different when comparing the control and RT3DTEE groups (nonsignificant interaction). On bivariate analysis, both ablation time and group were significantly (both p values <0.001) and independently associated with fluoroscopy time and dose, with markedly lower values for the RT3DTEE group.

As experience with RT3DTEE increased, procedural and fluoroscopy times further reduced in the last 10 cases compared with the first 10 cases, thus indicating a strong learning curve effect (Table 2, Fig. 6). Of note, significant reduction of RFA time was observed in the last RT3DTEE subgroup (median 7.0 min, IQR 6.4 to 8.4 min) compared

Table 1. Patient Baseline Characteristics

Characteristic	Conventional (n = 49)	RT3DTEE (n = 21)
Men	41	18
Age (yrs)	68.3 ± 9.4	61.3 ± 12.5*
Hypertension	29	9
Coronary artery disease	24	6
Valve disease	6	3
Other CV disease	13	6
"Lone" atrial flutter	6	3
COPD	3	2
Left atrial diameter (mm)	43.8 ± 9.4	43.5 ± 8.9
LVEF (%)	48.9 ± 17.3	56.4 ± 13.2
Paroxysmal atrial flutter	18	11
Persistent atrial flutter	30	11
History of atrial fibrillation	15	14†
Treatment with AA drugs		
Amiodarone	15	4
Sotalol	3	1
Class IC AA drugs	1	1
Beta-blockers	30	15
Digitalis	2	0
Calcium channel blockers	1	0
ACE inhibitors/ARBs	30	11
Diuretic agents	21	4
Statins	27	7

Values are n or mean ± SD. *Significant difference for age (p = 0.02). †Difference in the prevalence of atrial fibrillation (p = 0.03).
AA = antiarrhythmic; ACE = angiotensin-converting enzyme; ARB = angiotensin receptor blocker; CV = cardiovascular; COPD = chronic obstructive pulmonary disease; LVEF = left ventricular ejection fraction; RT3DTEE = real-time 3-dimensional transesophageal echocardiography.

with the control group (median 11.7 min, IQR 8.0 to 20.0 min) (p = 0.036). In 8 of the 9 patients (89%) with complex CVTI anatomy (multiple prominent features), CVTI conduction block was obtained by ablating along the inferolateral isthmus line.

No major or minor complications ensued from the ablation procedure in either group.

DISCUSSION

To the best of our knowledge, ours is the first study to systematically evaluate the use of RT3DTEE to guide a transcatheter ablation procedure, and it may therefore be considered as a proof of concept for the use of RT3DTEE in guiding RFA of atrial arrhythmias. RT3DTEE reliably visualized the CVTI in nearly all patients, providing enough temporal and spatial resolution for tracking ablation catheter movements, thus enabling successful treatment of CVTI-dependent atrial flutter ablation in all patients. In comparison with the conventional fluoroscopy-guided approach, RT3DTEE was equally effective in achieving conduction block across the CVTI, with a smaller number of RF applications, and entailed a significant reduction of radiation exposure and procedural time.

Anatomical characterization of the CVTI in patients with typical common atrial flutter. Anatomic data on the CVTI from autopsy (13) and from cardiac computed tomographic (14) evaluations in general patient cohorts without specific atrial arrhythmic conditions have described a high anatomical heterogeneity of this structure. More specifically, data on the characterization of CVTI anatomy in patients with common atrial flutter are derived mostly from angiography of the right atrium (15,16). The major advantage of RT3DTEE is the ability to precisely evaluate anatomical and morphological characteristics in vivo and in real time. In the patient cohort of this study with atrial flutter, RT3DTEE confirmed that the CVTI is a complex and heterogenous structure. The incidence of prominent Eustachian ridge and valve (60%) was greater than in the general population (20% [14]) but in line with other studies performed in patients with common atrial flutter (15). Moreover, in this study, prominent Eustachian ridge and valve, a medial recess, and the presence of pectinate muscles sometimes coexisted (20%). This finding emphasizes that structural and morphological heterogeneity may represent an important arrhythmogenic substrate for triggering and maintaining macroreentry.

Improving navigation along the CVTI while reducing procedural time. Constant efforts have been oriented toward rendering procedural time for CVTI ablation more predictable (3–7,15,17–22) (Table 4). A number of studies have explored the importance of adequate structural characterization through either angiography (15,16), magnetic resonance imaging (7,23), or the use of nonfluoroscopic mapping techniques (5,6,21). Assessment of remote magnetic navigation has also been investigated, yielding

Table 2. Distribution of Prominent CVTI Anatomical Features in All Patients (n = 20) and Divided According to the Two Patient Subgroups (First 10 and Last 10 Patients) Treated With the RT3DTEE-Guided Approach

Anatomical Feature	All Patients	First 10	Last 10
Long CVTI	11	6	5
Prominent Eustachian ridge	9	3	6
Prominent Eustachian valve	6	4	2
Deep septal recess	8	5	3
Presence of pectinate muscle	10	3	7
Patients with 3 or more features	9	5	4

CVTI = cavotricuspid isthmus; RT3DTEE = real-time 3-dimensional transesophageal echocardiography.

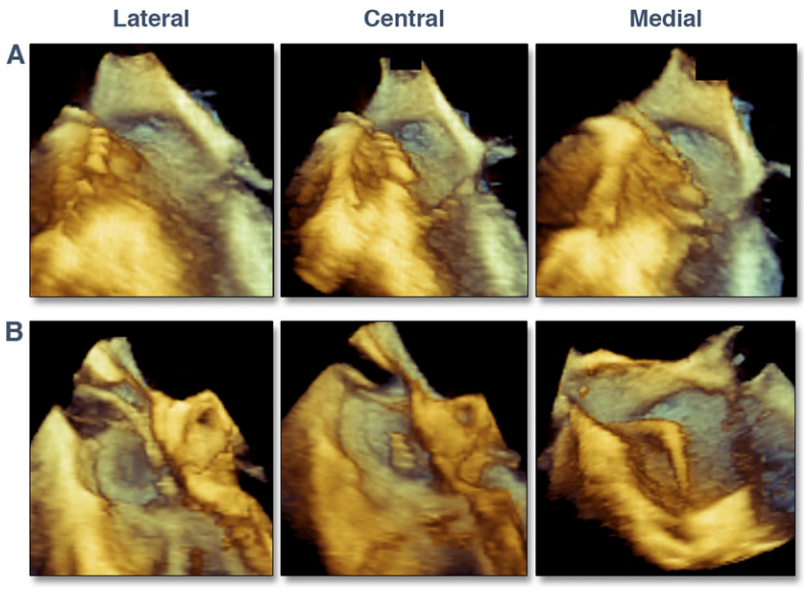

Figure 4. Visualization of Ablation Catheter Contact and Localization

The catheter is viewed along the lateral, central, and medial portions of the cavotricuspid isthmus **(A)**. **(B)** Differences between gold-tip ablation catheter, with closely intercalated electrodes **(left)**, and platinum-iridium catheter from a different manufacturer **(middle)** may be appreciated. Please see Online Video 1.

only modest results, because this technique, while reducing radiation exposure, increases RF application time (3,4).

RT3DTEE allowed the simultaneous and immediate characterization of the CVTI, and in most cases with complex "septal" anatomy (8 of 20 patients), an inferolateral line was performed to obtain CVTI block (Fig. 7, Online Video 2) (14,16,24,25). A prominent Eustachian valve was almost always associated with a prominent Eustachian ridge. Other important obstacles were considered to be the length of the isthmus (7,15,22) as well as the CVTI–to–inferior vena cava angle (7). With regard to the latter feature, our preliminary experience with nonquantitative RT3DTEE did not assess the CVTI–to–inferior vena cava angle in real time.

As observed, the learning curve associated with the novel approach played a role. This was shown by reduced dispersion of procedural times, radiation exposure, and ablation times, defined as a narrowing of the IQR around the median values in the latter cases (Fig. 6). This suggests that RT3DTEE may render procedural time highly predictable and RF delivery more precise, because ablation of the CVTI is performed by circumventing anatomic obstacles.

Reduction of biological risk from radiation exposure. The excitement generated by cardiovascular imaging has recently been tempered by a string of high-impact publications (26–30) that have raised concerns about increased medical procedure radiation exposure and the potential risk for cancer. Most atrial arrhythmias are not life threatening, and the procedural purpose is mostly

Table 3. Procedural Data

Variable	Conventional (n = 49)	RT3DTEE (n = 20)	p Value
Total procedural time (min)	115.0 (85.0–133.0)	73.0 (60.0–91.0)	<0.001
Fluoroscopy time (min)	19.3 (12.9–36.0)	4.2 (3.1–8.4)	<0.001
Fluoroscopy dose (cGy·cm^2)	3,520.7 (1,700.0–6,709.0)	575.4 (438.5–1,299.4)	<0.001
Number of RF applications	12 (10–22)	7 (6–10)	0.007
Ablation time (min)	11.7 (8.0–20.0)	8.7 (6.5–14.6)	0.145

Values are median (interquartile range).
RF = radiofrequency; RT3DTEE = real-time 3-dimensional transesophageal echocardiography.

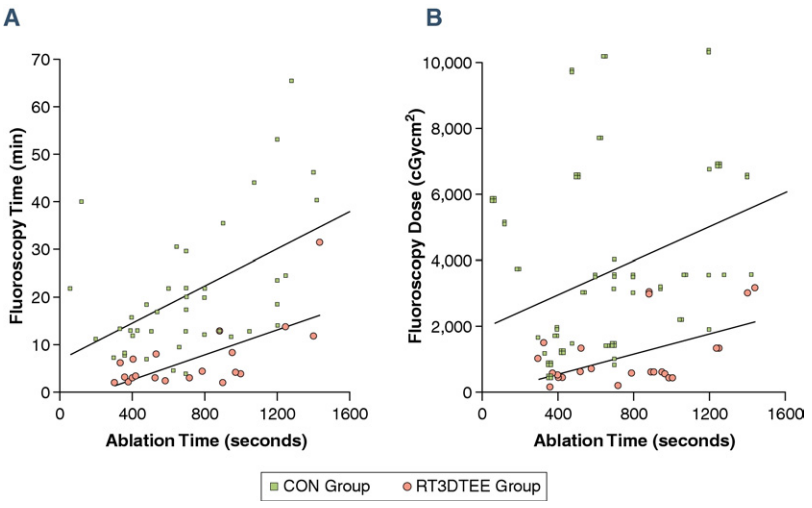

Figure 5. Plotting of Procedural Data of the Two Study Groups

For real-time 3-dimensional transesophageal echocardiography (RT3DTEE) **(red circles)** and control (CON) **(green squares)** groups, fluoroscopy time **(A)** and dose **(B)** are correlated to ablation time.

improvement in quality of life. In this view, the potential curative intent should be weighed against procedural success rate, risk for complications, and the long-term risk for a biological effect. Thus, following the principle of "as low as reasonably achievable," which has guided the U.S. Food and Drug Administration's approval process and developments in the field of cardiac imaging, our data show that RT3DTEE may well serve this goal (31). RT3DTEE resulted in at least a 3-fold

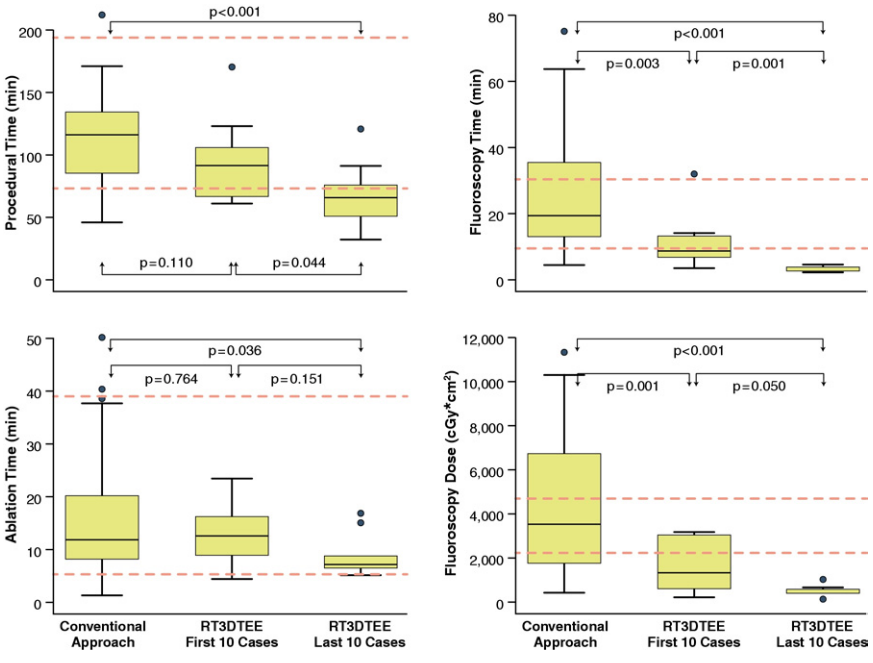

Figure 6. Box Plot for Procedural Data

Midline: median; **box:** 25th to 75th percentiles; **whiskers:** nonoutlier extremes; **dots:** outlier values. **Upper and lower horizontal dashed red lines** refer to the highest and lowest mean values from published research (for details, refer to Table 4). RT3DTEE = real-time 3-dimensional transesophageal echocardiography.

Table 4. Principal Procedural Data Derived From Other Studies on CVTI Ablation Using the Conventional Fluoroscopy-Guided Approach With an 8-mm RFA Catheter

Study (Ref. #)	n	Procedure Time (min)	Fluoroscopy Time (min)	Fluoroscopy Dose (cGy·cm^2)	RF Application Time (min)	Number of RF Applications
Kottkamp et al. (5)	24	75 ± 27	22 ± 6.3		15.0 ± 6.2	10 ± 5
Willems et al. (6)	40	172.5 ± 47.4	29.2 ± 9.4			16.7 ± 6.5
Heidbüchel et al. (15)	100	119 ± 50	26 ± 14.8			2.3 ± 2.5
Schreieck et al. (17)	50	/	15.7 ± 10.7		39 ± 27	12.9 ± 8.6
Schneider et al. (18)	24	/	15.9 ± 10.6	2,100 ± 1,980		
Da Costa et al. (22)	281	72 ± 26	14.3 ± 13.0		15.0 ± 15.0	
Steven et al. (3)	25	79.2 ± 30.6	8.2 ± 4.6		5.4 ± 3.6	
Kim et al. (19)	183	197 ± 45	45 ± 25			
Hindricks et al. (21)	105	88 ± 54	14.8 ± 11.9			
Vollmann et al. (4)	45	77 ± 24	15.0 ± 4.1	4,303 (3,435–5,862)	7.5 ± 3.4	9 (6–16)
Kirchhof et al. (7)	26	195 ± 19	29.0 ± 4.0		21.0 ± 7.0	14 (2–41)
Kardos et al. (20)	16	73.1 ± 15	7.1 ± 3.8		8.0 ± 5.2	6.6 ± 3.1

Values are n, mean ± SD, or median (interquartile range).
CVTI = cavotricuspid isthmus; RF = radiofrequency; RFA = radiofrequency ablation.

reduction in radiation exposure compared with the conventional fluoroscopy-assisted approach.

The reduction in fluoroscopy time observed during RT3DTEE was greater than that obtained with either the remote magnetic (3,4) or the electroanatomically guided (21) approach. In the latter case, mean fluoroscopy time was approximately 8 min, and as with RT3DTEE, the use of fluoroscopy was limited to the diagnostic part of the procedure, whereas ablation was guided mainly by navigation without fluoroscopy.

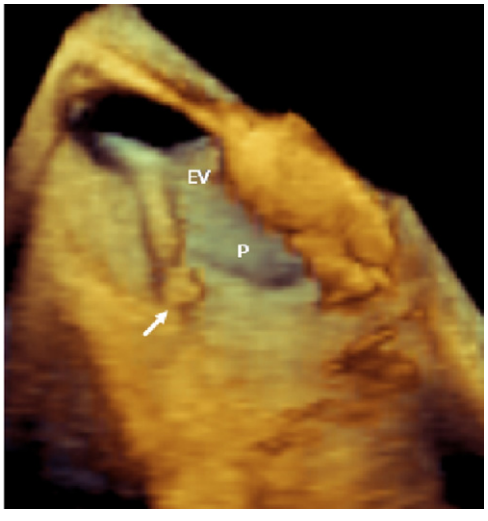

Figure 7. Radiofrequency Ablation in the Presence of a Septal Recess

In some cases with prominent septal recesses, radiofrequency energy delivery was applied by targeting the lateral border of the recess, and cavotricuspid isthmus conduction block was subsequently obtained. See Online Video 2. EV = Eustachian valve; P = septal pouch.

Issues and challenges in the use of RT3DTEE for monitoring catheter ablation procedures. The findings of this study substantiate the expanding role of RT3DTEE from a diagnostic modality to a tool for monitoring invasive procedures. Compared with other interventional cardiologic procedures (percutaneous valve repair or replacement, closure of atrial and ventricular defects, left atrial appendage closure), standard electrophysiological and ablation procedures possess many particularities. The relatively rapid catheter movement, the relatively narrow visualization field at an acceptable high frame rate (25 Hz), and metallic artifacts due to the large catheter tip may all represent technical challenges for routine adoption of the technique. In addition, the finding that different ablation catheter manufacturers present different acoustic impedance suggests that some catheters are more ultrasound compatible than others; this issue merits further investigation. Despite these challenges and the burden involved in using RT3DTEE to monitor an electrophysiological procedure, there are certain situations, such as pregnancy or in younger patients, in which a strong incentive to reduce harmful radiation exposure while minimizing procedural risks exists. To this end, the finding that RT3DTEE may reliably and effectively monitor an ablation procedure with only a short associated learning curve may be interesting and helpful. Finally, RT3DTEE may provide a unique way to further define key anatomical structures responsible for a macroreentry in the CVTI region.

Study limitations. This study was a pilot, single-center, nonrandomized study with a relatively small patient population. The RT3DTEE approach was represented by the need for general anesthesia, which lengthened overall procedural duration and could potentially increase risk; such a limitation may be overcome in the future when small-sized transesophageal echocardiographic probes become available (32). Also, general anesthesia and the use of mild sedation and pain control medication in the conventional approach to limit patient pain and movement may each have effects on procedural outcome data. For this reason, in the computation of the number of RF lesions and time of ablation, only RF applications lasting ≥60 s were considered.

RT3DTEE assessment of CVTI anatomy was mostly qualitative. Clearly, a validation process with other imaging modalities is needed. Despite some modest baseline differences between the 2 study groups, it is unlikely that these may have influenced acute procedural outcomes. More studies are needed to establish correlates between CVTI anatomical and morphological features, clinical variables, and their influence on CTVI ablation.

CONCLUSIONS

This study has demonstrated that RT3DTEE-guided ablation of the CVTI is feasible, yielding comparable acute efficacy to the standard fluoroscopy-guided approach. This imaging modality conferred high-resolution images, allowing navigation without fluoroscopy and precise RF delivery in target anatomical areas of the CVTI, thus allowing considerable reductions of procedural time, radiation exposure, and the number of RFA applications. Further investigations are needed to explore this new promising anatomically driven, fluoroscopy-free navigation approach for guiding the ablative treatment of cardiac arrhythmias.

Reprint requests and correspondence: Dr. Angelo Auricchio, Division of Cardiology, Fondazione Cardiocentro Ticino, Via Tesserete 48, CH-6900 Lugano, Switzerland. *E-mail: angelo.auricchio@cardiocentro.org.*

REFERENCES

1. Blomström-Lundqvist C, Scheinman MM, Aliot EM, et al. ACC/AHA/ESC guidelines for the management of patients with supraventricular arrhythmias—executive summary: a report of the American College of Cardiology/American Heart Association Task Force on Practice Guidelines and the European Society of Cardiology Committee for Practice Guidelines (Writing Committee to Develop Guidelines for the Management of Patients With Supraventricular Arrhythmias). J Am Coll Cardiol 2003;42:1493–531.
2. Pérez FJ, Schubert CM, Parvez B, Pathak V, Ellenbogen KA, Wood MA. Long-term outcomes after catheter ablation of cavo-tricuspid isthmus dependent atrial flutter: a meta-analysis. Circ Arrhythm Electrophysiol 2009;2:393–401.
3. Steven D, Rostock T, Servatius H, et al. Robotic versus conventional ablation for common-type atrial flutter: a prospective randomized trial to evaluate the effectiveness of remote catheter navigation. Heart Rhythm 2008;5:1556–60.
4. Vollmann D, Lüthje L, Seegers J, Hasenfuss G, Zabel M. Remote magnetic catheter navigation for cavotricuspid isthmus ablation in patients with common-type atrial flutter. Circ Arrhythm Electrophysiol 2009;2:603–10.
5. Kottkamp H, Hügl B, Krauss B, et al. Electromagnetic versus fluoroscopic mapping of the inferior isthmus for ablation of typical atrial flutter: a prospective randomized study. Circulation 2000;102:2082–6.
6. Willems S, Weiss C, Ventura R, et al. Catheter ablation of atrial flutter guided by electroanatomic mapping (CARTO): a randomized comparison to the conventional approach. J Cardiovasc Electrophysiol 2000;11:1223–30.
7. Kirchhof P, Ozgün M, Zellerhoff S, et al. Diastolic isthmus length and "vertical" isthmus angulation identify patients with difficult catheter ablation of typical atrial flutter: a pre-procedural MRI study. Europace 2009;11:42–7.
8. Efstathopoulos EP, Katritsis DG, Kottou S, et al. Patient and staff radiation dosimetry during cardiac electrophysiology studies and catheter ablation procedures: a comprehensive analysis. Europace 2006;8:443–8.
9. Faletra F, Ho SW, Auricchio A. Anatomy of right atrial structures by real-time 3-dimensional transesophageal echocardiography. J Am Coll Cardiol Img 2010;3:966–75.
10. Balzer J, Kelm M, Kühl HP. Real-time three-dimensional transoesophageal echocardiography for guidance of non-coronary interventions in the catheter laboratory. Eur J Echocardiogr 2009;10:341–9.
11. Tada H, Oral H, Sticherling C, et al. Double potentials along the ablation line as a guide to radiofrequency ablation of typical atrial flutter. J Am Coll Cardiol 2001;38:750–5.
12. Cauchemez B, Haissaguerre M, Fischer B, Thomas O, Clementy J, Coumel P. Electrophysiological effects of catheter ablation of inferior vena cava-tricuspid annulus isthmus in common atrial flutter. Circulation 1996;93:284–94.
13. Gami AS, Edwards WD, Lachman N, et al. Electrophysiological anatomy of typical atrial flutter: the posterior boundary and causes for difficulty with ablation. J Cardiovasc Electrophysiol 2010;21:144–9.
14. Saremi F, Pourzand L, Krishnan S, et al. Right atrial cavotricuspid isthmus: anatomic characterization with multidetector row CT. Radiology 2008;247:658–68.
15. Heidbüchel H, Willems R, van Rensburg H, Adams J, Ector H, Van de Werf F. Right atrial angiographic evaluation of the posterior isthmus: relevance for ablation of typical atrial flutter. Circulation 2000;101:2178–84.

16. Da Costa A, Faure E, Thévenin J, et al. Effect of isthmus anatomy and ablation catheter on radiofrequency catheter ablation of the cavotricuspid isthmus. Circulation 2004;110:1030–5.
17. Schreieck J, Zrenner B, Kumpmann J, et al. Prospective randomized comparison of closed cooled-tip versus 8-mm-tip catheters for radiofrequency ablation of typical atrial flutter. J Cardiovasc Electrophysiol 2002;13:980–5.
18. Schneider MA, Ndrepepa G, Dobran I, et al. LocaLisa catheter navigation reduces fluoroscopy time and dosage in ablation of atrial flutter: a prospective randomized study. J Cardiovasc Electrophysiol 2003;14:587–90.
19. Kim AM, Turakhia M, Lu J, et al. Impact of remote magnetic catheter navigation on ablation fluoroscopy and procedure time. Pacing Clin Electrophysiol 2008;31:1399–404.
20. Kardos A, Foldesi C, Mihalcz A, Szili-Torok T. Cavotricuspid isthmus ablation with large-tip gold alloy versus platinum-iridium-tip electrode catheters. Pacing Clin Electrophysiol 2009;32 Suppl:S138–40.
21. Hindricks G, Willems S, Kautzner J, et al., for the EuroFlutter Investigators. Effect of electroanatomically guided versus conventional catheter ablation of typical atrial flutter on the fluoroscopy time and resource use: a prospective randomized multicenter study. J Cardiovasc Electrophysiol 2009;20:734–40.
22. Da Costa A, Romeyer-Bouchard C, Dauphinot V, et al. Cavotricuspid isthmus angiography predicts atrial flutter ablation efficacy in 281 patients randomized between 8 mm- and externally irrigated-tip catheter. Eur Heart J 2006;27:1833–40.
23. Hoffmann BA, Koops A, Rostock T, et al. Interactive real-time mapping and catheter ablation of the cavotricuspid isthmus guided by magnetic resonance imaging in a porcine model. Eur Heart J 2010;31:450–6.
24. Asirvatham SJ. Correlative anatomy and electrophysiology for the interventional electrophysiologist: right atrial flutter. J Cardiovasc Electrophysiol 2009;20:113–22.
25. Scaglione M, Caponi D, Di Donna P, et al. Typical atrial flutter ablation outcome: correlation with isthmus anatomy using intracardiac echo 3D reconstruction. Europace 2004;6:407–17.
26. Faletra FF, D'Angeli I, Klersy C, et al. Estimates of lifetime attributable risk of cancer after a single radiation exposure from 64-slice computed tomographic coronary angiography. Heart 2010;96:927–32.
27. Laskey WK, Feinendegen, LE, Neumann RD, Dilsizian V. Low-level ionizing radiation from noninvasive cardiac imaging: can we extrapolate estimated risks from epidemiologic data to the clinical setting? J Am Coll Cardiol Img 2010;3:517–24.
28. Gerber TC, Gibbons RJ. Weighing the risks and benefits of cardiac imaging with ionizing radiation. J Am Coll Cardiol Img 2010;3:528–35.
29. Halliburton SS, Schoenhagen P. Cardiovascular imaging with computed tomography responsible steps to balancing diagnostic yield and radiation exposure. J Am Coll Cardiol Img 2010;3:536–40.
30. Shaw LJ, Achenbach S, Chandrashekhar Y, et al. Imaging modalities and radiation: benefit has its risks. . . . J Am Coll Cardiol Img 2010;3:250–2.
31. U.S. Food and Drug Administration, Center for Devices and Radiological Health. Whole body scanning using computed tomography (CT): what are the radiation risks from CT? Available at: http://www.fda.gov/cdrh/ct/risks.html. Accessed July 20, 2006.
32. Stec S, Zaborska B, Sikora-Frac M, Krynski T, Kulakowski P. First experience with microprobe transoesophageal echocardiography in non-sedated adults undergoing atrial fibrillation ablation: feasibility study and comparison with intracardiac echocardiography. Europace 2011; 13:51–6.

Key Words: atrial flutter ablation ■ cavotricuspid anatomy ■ electrophysiologic imaging ■ 3-dimensional echocardiography.

APPENDIX

For supplementary videos and their legends, please see the online version of this article.